Studies of Quantum Entanglement in 100 Dimensions

Mario Krenn[1,2], Marcus Huber[3,4,5], Robert Fickler[1,2], Radek Lapkiewicz[1,2], Sven Ramelow[1,2], Anton Zeilinger[1,2]

[1]*Institute for Quantum Optics and Quantum Information (IQOQI), Austrian Academy of Sciences, Boltzmanngasse 3, A-1090 Vienna, Austria.*
[2]*Vienna Center for Quantum Science and Technology (VCQ), Faculty of Physics, University of Vienna, Boltzmanngasse 5, A-1090 Vienna, Austria.*
[3]*University of Bristol, Department of Mathematics, Bristol BS8 1TW, U.K.*
[4]*ICFO-Institut de Ciencies Fotoniques, E-08860 Castelldefels (Barcelona), Spain.*
[5]*Fisica Teorica: Informacio i Fenomens Quantics, Departament de Fisica, Universitat Autonoma de Barcelona, E-08193 Bellaterra (Barcelona), Spain.*

Correspondence to M.K. (mario.krenn@univie.ac.at) or A.Z. (anton.zeilinger@univie.ac.at)

Entangled quantum systems have properties that have fundamentally overthrown a classical worldview [1, 2]. Increasing the complexity of entangled states by expanding their dimensionality not only allows the implementation of novel fundamental tests of nature [3, 4], but also enables genuinely new protocols for quantum communication [5-7] and quantum computation [8]. In our experiment we generate photons entangled in angular momentum and radial modes. We unambiguously verify that these photons are highly entangled in most 2x2-dimensional subspaces of a 34.500-dimensional Hilbert space, which suggests the generation of genuine high dimensional entanglement. We develop a source-independent criterion that reveals an entanglement dimensionality of over 100. For the criterion we propose a mathematical conjecture for which we have strong numerical evidence and theoretical arguments. Furthermore, the size of the entangled Hilbert space is of the same magnitude as the largest entangled multipartite systems experimentally measured so far. This result indicates the great potential of high-dimensional entangled photons for a wide range of quantum information tasks.

It has been shown that the dimensionality of the quantum system is particularly important for quantum computation. While any continuous measure of entanglement can be arbitrarily small, a sufficiently high dimensionality of entanglement is necessary for any quantum speed up [9-11]. Therefore generating and verifying genuine high-dimensional entanglement has been a main focus of experiments performed in quantum optics.

One method of bipartite high-dimensional entanglement, namely spatial modes of photons, has attracted much attention in recent years [12, 13]. The spatial mode entanglement is readily available from non-linear processes in optical crystals, and theoretically its dimensionality can be arbitrarily high. Therefore a natural question is “what is the actual dimensionality of entanglement” or “how many degrees of freedom are entangled in the quantum state?”. Several experiments aimed to answer that question with different methods.

An interesting example is the violation of a 12-dimensional generalized Bell-inequality. This was possible by assuming conservation of orbital angular momentum (OAM) and numerical maximization of dimensionality bounds [13]. With a different method, the capability of revealing dimensionality with non-perfect measurements was analyzed. By assuming pure states, the authors showed the potential of revealing a dimensionality of about 50 [14, 15]. In yet another experiment it was demonstrated that by thoughtfully optimizing the OAM-spectrum, entanglement of up to 30 dimensions can be achieved. This was possible by applying a dimensionality criterion that assumes pure states as well [16].

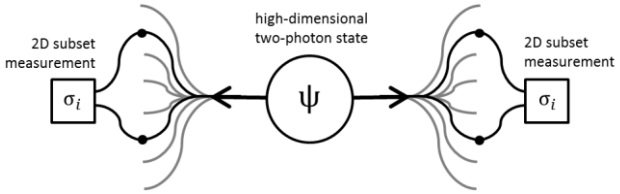

Figure 1: Visualization of the measurement concept. The two photons are separated into different paths. Each of the photons is in a superposition of many modes. We perform the same two-dimensional subspace measurement on both photons. When we consider all two-dimensional subspaces, we can determine the dimensionality of entanglement. As there are three 2-dimensional Pauli matrices, and each Pauli matrix requires 2 projective measurements on each of the two photons, we perform 12 measurements per two-dimensional subspace.

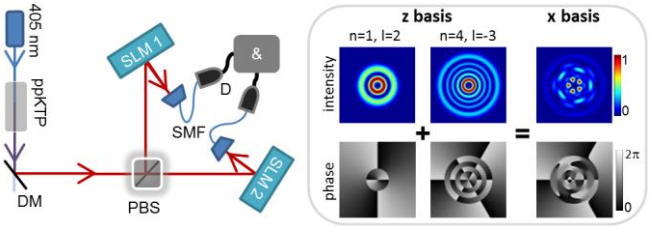

Figure 2: Schematic of the experimental setup. We pump a type-II quasi phase-matched nonlinear periodically poled potassium titanyl phosphate (ppKTP) crystal with a 405 nm, 60mW single-mode laser. Spontaneous parametric down-conversion creates photon pairs with 810 nm wavelength and orthogonal polarization. We remove the pump beam at a dichroic mirror (DM) and separate the two photons at a polarizing beam splitter (PBS). In both arms of the setup we use spatial light modulators (SLM) to perform a mode-transformation of the photons. The transformation done by a computer-generated hologram at the SLM converts a specific mode into the Gauss mode. Only the Gauss mode couples into a single mode fiber (SMF), thus the SLM+SMF act as a mode filter. In the end, we detect the photons with avalanche photo-diode based single photon detector (D) and analyze the time correlation using a coincidence-logic (&). The inset shows an example of a two-dimensional subspace. The intensities and phases for two different modes in the z basis are demonstrated, and their superposition leads to a mode in the x basis.

In general, accessing and verifying genuine high order entanglement from unknown sources poses significant experimental and analytical challenges, because examining Schmidt numbers (which is the dimensionality of the entanglement) requires reliable access to the full density matrix. For example, in Hilbert spaces of dimension (200*200), this would correspond to more than 10^9 measurement settings accessing the full Hilbert space [17, 18]. To determine the dimensionality of entanglement, dimension witnesses provide an experimentally feasible method [13, 19]. Generally a dimension witness defines a set of measurements and gives a bound of the experimental result depending on the dimensionality of entanglement. Such methods can reveal the Schmidt number of a state with just a fraction of measurements compared to full state tomography. A similar concept has been employed to analyze the dimension of the underlying Hilbert-space, using high-dimensional entanglement [20, 21].

In our experiment, we reveal high dimensional entanglement in a completely state independent way (i.e. no assumptions need to be made about the quantum state under investigation, such as purity). This is achieved by developing a novel nonlinear entanglement dimension criterion. The witness is capable of unambiguously revealing high dimensional entanglement through sub-space correlations (see supplementary). In our case, we analyze correlations in two-dimensional subspaces (Figure 1).

Although individually these virtual two-qubit systems can never reveal more than mere qubit entanglement [18], we explicitly show how their combination can be exploited to reveal the full dimensionality of entanglement in arbitrarily large Hilbert spaces.

We find bounds for these correlations (assuming a mathematical statement for which we have strong numerical evidences and theoretical arguments, see supplementary material). The number of measurements required to extract the dimensionality information is always less than for quantum state tomography and is generally less than required for the violation of generalized Bell-inequalities [18]. To fully access the dimensionality of a (186*186)-dimensional Hilbert space, we only required ~51.000 measurement settings (with ~205.000 projective measurements). This constitutes ~0,005% of a full state tomography.

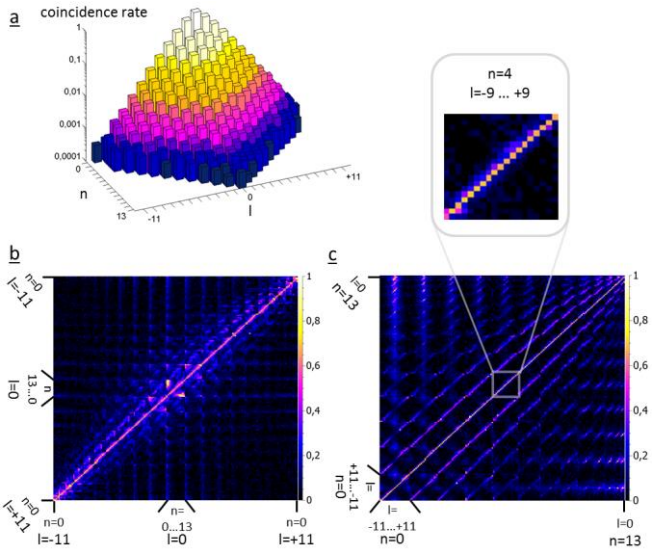

Figure 3: a) Normalized coincidence rate of different modes (with logarithmic scale), depending on the two mode numbers ("full-field"-bandwidth). The probability for higher modes drops fast, therefore a logarithmic scale has been used. b) Weighted correlations between different modes. Due to different probabilities of different modes, we weight every correlation with the probability of involved modes. That means, $\langle i \mid j \rangle_{weighted} = N \frac{\langle i \mid j \rangle_{measured}}{\sqrt{\langle i \mid i \rangle \langle j \mid j \rangle}}$, where *i* and *j* stand for different modes, and N is a normalization constant. Thereby the visualization of correlations and anti-correlations is more informative (without weighting, only a few bright spots would be visible due to the different count rates for different modes). The two pictures show different sorting of the two quantum numbers, thus different properties of the state. The modes are sorted first by the l number, then modes with same l numbers are sorted by n. The anti-correlation between different l-modes can be seen very clearly. The central square, which corresponds to l=0, contains bright spots on the edges. They are artifacts of the approximate holograms used in the projections, strongly enhanced by the weighting. c) The modes (weighted in the same way as before) are sorted first by the n number, then by l. (For example: In the inset, the correlations of modes with n=4 are displayed. The remaining 19 different settings (l=-9 … +9) are sorted ascending.) The off-diagonals indicate that n-modes are not as well correlated as l-modes.

Entanglement in our experiment is analyzed in the Laguerre-Gauss (LG) basis. The first mode number l describes the OAM states of light [22-24]. The second index n corresponds to the number of radial rings in the intensity profile. Lately this second degree of freedom has been analyzed theoretically in a quantum mechanical framework [25]. In a recent experiment correlations were shown for the first time in both mode numbers, revealing their potential to access even higher-dimensional entanglement [26].

In our setup, we create photon pairs in a non-linear crystal, and analyze their spatial mode structure using holographic transformations (more details in Figure 2). We analyzed the set of modes with the highest count rates. The maximal OAM value was l=+/-11 (for n=0), and the maximal radial mode number was n=13 for l=0 (Figure 3).

In our experiment, we measured visibilities in three mutually unbiased bases (MUBs, i.e. visibility=$\left\langle \sigma_i \otimes \sigma_i \right\rangle$, i={x,y,z}, σ_i denote the single-qubit Pauli matrices) in every two-dimensional subspace of a (186*186)-dimensional Hilbert-space. This results in 17.205 subsets with 206.460 projective measurements in total.

From the resulting set of correlations we can analyze the „full-field"-bandwidth (which consists of the spiral and radial bandwidth) of our down-conversion state (Figure 3a). The correlations in the z-basis between the 186 modes can be observed in Figure 3.

The three visibilities of the two-dimensional subspace characterize the amount of entanglement between the two modes. In figure 4, we analyse the sum of visibilities in two-dimensional subspaces and observe regions of modes that have higher (average) visibilities. This effect can be explained by the different generation probability of modes (see figure 3), which leads to non-maximally entangled states with small visibility in the x- and y-basis. In general, modes with similar probabilities have a high visibility in all bases.

To extract the information about the dimensionality of entanglement, we use a novel non-linear entanglement witness. It is the sum of all visibilities of the three MUBs in all two-dimensional subspaces

$$\left\langle \hat{W} \right\rangle = \sum_{a=0}^{D-2} \sum_{b=a+1}^{D-1} \frac{1}{N_{a,b}} \left(\left\langle \sigma_x^{a,b} \otimes \sigma_x^{a,b} \right\rangle + \left\langle \sigma_y^{a,b} \otimes \sigma_y^{a,b} \right\rangle + \left\langle \sigma_z^{a,b} \otimes \sigma_z^{a,b} \right\rangle \right), \quad (1)$$

where a and b stand for specific $LG_{n,l}$ modes, D stands for the number of modes considered for the witness. $N_{a,b}$ is a normalization constant that appears because by measuring a two-dimensional subspaces, we ignore all the other modes. It can be shown that the normalized subspace-witness can reveal higher Schmidt numbers than its linear form in the case of non-maximal entangled states (which is the case for our experiment, as one can see in figure 3).

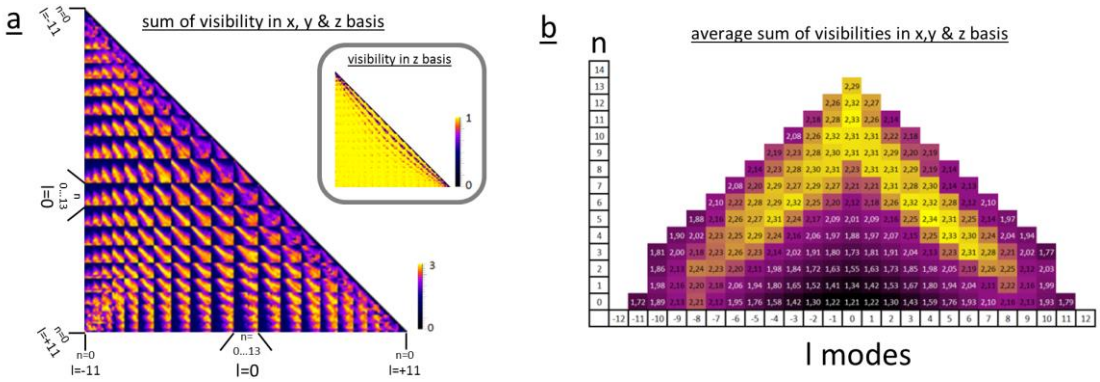

Figure 4: Sum of coincidence visibilities in x, y and z basis of 17.205 two-dimensional subspaces. a) This picture shows the sum of the three visibilities for every two-dimensional subspace, with the same mode-sorting as in figure 3b. The structure originates from different count rates for different modes, which leads to non-maximally entangled states and a smaller overall visibility in the corresponding two-dimensional subspace. The visibility in the z-basis is not affected by the non-maximal entanglement, as shown in the inset. However, the visibilities in x- and y-basis are very small for strongly asymmetric probabilities. b) The average sum of visibilities (in x, y, and z basis) of a specific mode with all other modes is indicated. The observable structure originates again from non-maximally entanglement due to different count rates. The bright regions in the center are modes with a similar probability. The central low-order modes (such as the Gauss mode) have the highest probability (Figure 3), therefore the lowest average visibility. Precisely, the Gauss mode has an average sum of visibilities of 1,21 – which mainly results from the visibilities in z-basis. A maximally entangled high-dimensional state would have a summed visibility of 3 for every mode.

We have analytically derived bounds for arbitrary Schmidt numbers and D on this correlation function for non-normalized subspaces. Using these results we were able to prove analytical and tight bounds for equally distributed subspaces. Strong numerical evidence suggests that this function (which is symmetric in its inputs) is indeed maximized by symmetric distributions of the subspaces. This is one of the reasons (others can be found in the supplementary) why we suggest that the derived bounds are actually the global maximum, that can be attained for a mixture of maximally entangled pure states. The entanglement dimensionality bounds can be written as

$$\left\langle \hat{W} \right\rangle \leq Dd + \frac{D(D-3)}{2}, \tag{2}$$

where d is the dimensionality of an arbitrary entangled quantum state (i.e. the Schmidt number). The left side of the inequality represents the measured value of equation (1). The right side denotes the maximal value which can be obtained by a d-dimensional entangled state. If the measurement result exceeds the value for an d-dimensional entangled state, we know that the considered state was entangled in at least (d+1) dimensions. The bounds are therefore sufficient but not necessary (i.e. we have at least (d+1) dimensional entanglement, but we could have even more).

When we consider the whole 186-dimensional Hilbert-space, we obtain

$$\left\langle \hat{W} \right\rangle_{D=186} = 35\,529 \pm 6, \tag{3}$$

which corresponds to 100-dimensional entanglement (101dim: W>35.619; 100dim: W>35.433; 99dim: W>35.247). The confidence interval here (and elsewhere) corresponds to one standard deviation.

As shown in Figure 4, some modes contribute more to the witness than others. Since the bounds of the witness depend on the number of modes considered, we can search for the subspace with the highest-dimensional entanglement. By removing 19 modes with the smallest contribution to the witness (i.e. not considering the corresponding two-dimensional subsets of those modes) we obtain

$$\left\langle \hat{W} \right\rangle_{D=167} = 30\,836 \pm 6, \tag{4}$$

which correspond to a 103-dimensional entanglement (104dim: W>30.895; 103dim: W>30.728; 102dim: W>30.561).

Our results are state-independent, we don't require any knowledge about the considered quantum state. As a comparison, if we had assumed properties of the state such as purity, we could fully analytical derive different bounds for the witness in (1), and find more than 140-dimensional entanglement.

In summary, we analyzed the dimensionality of entanglement of a two-photon state generated in down-conversion. Both quantum numbers of Laguerre-Gauss modes have been considered to obtain high dimensionality. We developed an entanglement witness for arbitrary high dimensions which does not require any a priori knowledge about the analyzed state. This allowed us to analyze a state in a Hilbert space of (186*186) dimensions with only ~205.000 projective measurements. We verified that the analyzed state was entangled in at least 103 dimensions (assuming the mathematical statement mentioned before, for which we have theoretical arguments and strong numerical evidence). The size of the entangled Hilbert-space is of the same magnitude than the biggest quantum systems with multipartite entanglement measured so far, such as 14-qubit ion entanglement [27].

The entanglement dimensionality could be further increased by specially designed crystal parameters [28]. A different approach is the employing of additional degrees of freedom photons [29], or by considering a combination of multi-partite and multi-dimensional entanglement [30]. Additionally, the question about a generalization of the introduced entanglement dimension criterion is very interesting for experimentalists as well as for theorists: How can the proof of the bounds be completed fully analytical? How can the normalized subspace criterion be applied to high-dimensional multipartite systems? What additional information can be extracted from normalized subspaces?

We hope that this experimental result stimulates further theoretical investigations on how to exploit the potential of large entangled Hilbert spaces consisting of high-dimensionally entangled entities in novel ways (e.g. [7]).

Methods:
The holograms on the SLMs are calculated using a plane-wave approximation. This could lead to non-orthogonal projective measurements. However, for our system this effect can only reduce the visibilities thus reduce the observed dimensionality. We restrict ourselves to two-dimensional subspaces, as this leads to simpler holograms on the SLMs and increases the mode transformation accuracy due to the finiteness of the pixels. Furthermore this method allows us to treat non-maximally entangled state (Figure 2) directly, therefore we do not need to perform any entanglement concentration [13].

All confidence intervals have been calculated using Monte-Carlo simulations. The detected photon numbers are Poisson distributed, which leads to asymmetric distribution especially for low count rates. Analytical treatment of error propagation for such a big number of measurements was not feasible anymore.

Acknowlegdement
This work was supported by the ERC Advanced Grant No. 227844 "QIT4QAD"; SIQS, No. 600645 EU-FP7-ICT; and the Austrian Science Fund FWF with the SFB F40 (FoQus) and W1210-2 (CoQus). MH would like to acknowledge the MarieCurie IEF grant QuaCoCoS – 302021. MK would like to thank the quantum information theory groups at ICFO and UAB (Barcelona) and Christoph Schäff for interesting discussions, and MH for nice hospitality.

References:
[1] Einstein, A., Podolsky, B., & Rosen, N., Can Quantum-Mechanical Description of Physical Reality Be Considered Complete?. *Phys. Rev.* **47**, 777 (1935).

[2] Schrödinger, E., Discussion of probability relations between separated systems. *Proc. Camb. Phil. Soc.* **31**, 553 (1935).

[3] Yang T. *et.al.*, All-Versus-Nothing Violation of Local Realism by Two-Photon, Four-Dimensional Entanglement. *Phys. Rev. Lett.* **95**, 240406 (2005).

[4] Vértesi,T., Pironio, S., & Brunner, N., Closing the Detection Loophole in Bell Experiments Using Qudits. *Phys. Rev. Lett.* **104**, 060401 (2010).

[5] Gröblacher, S., Jennewein, T., Vaziri, A., Weihs, G., & Zeilinger A., Experimental quantum cryptography with qutrits. *New J. Phys.* **8**, 75 (2006).

[6] Molina-Terriza, G., Vaziri, A., Ursin, R., & Zeilinger A., Experimental Quantum Coin Tossing. *Phys. Rev. Lett.* **94**, 040501 (2005).

[7] Huber, M. & Pawlowski, M., Higher dimensional entanglement enables QKD without perfect randomness, *arXiv:1301.2455* (2013).

[8] Lanyon, B. P., *et.al.*, Simplifying quantum logic using higher-dimensional Hilbert spaces. *Nature Physics* **5**, 134 - 140 (2009).

[9] Jozsa, R., & Linden, N., On the role of entanglement in quantum-computational speed-up. *Proc. R. Soc. A* **459**, 2011 (2003).

[10] Vidal, G., Efficient Classical Simulation of Slightly Entangled Quantum Computations. *Phys. Rev. Lett.* **91**, 147902 (2003).

[11] Van den Nest, M., Universal Quantum Computation with Little Entanglement. *Phys. Rev. Lett.* **110**, 060504 (2013).

[12] Vaziri, A., Weihs, G., & Zeilinger, A., Experimental Two-Photon, Three-Dimensional Entanglement for Quantum Communication, *Phys. Rev. Lett.* **89**, 240401 (2002).

[13] Dada, A. C., Leach, J., Buller, G. S., Padgett, M. J., & Andersson, E., Experimental high-dimensional two-photon entanglement and violations of generalized Bell inequalities. *Nature Physics* **7**, 677–680 (2011).

[14] Pors, J. B., Shannon Dimensionality of Quantum Channels and Its Application to Photon Entanglement. *Phys. Rev. Lett.* **101**, 120502 (2008).

[15] Giovannini, D., Miatto, F. M., Romero, J., Barnett, S. M., Woerdman, J. P., & Padgett M. J., Determining the dimensionality of bipartite orbital-angular-momentum entanglement using multi-sector phase masks. *New Journal of Physics* **14**, 073046 (2012).

[16] Romero, J., Giovannini, D., Franke-Arnold, S., Barnett, S. M., & Padgett M. J., Increasing the dimension in high-dimensional two-photon orbital angular momentum entanglement. *Phys. Rev. A* **86**, 012334 (2012).

[17] Giovannini, D., Romero, J., Leach, J., Dudley, A., Forbes, A. & Padgett, M. J., Characterization of High-Dimensional Entangled Systems via Mutually Unbiased Measurements, *Phys. Rev. Lett.* **110**, 143601 (2013).

[18] Agnew, M., Leach, J., Boyd R. W., Observation of entanglement witnesses for orbital angular momentum states. *EPJ D* **66**, 156 (2012).

[19] Krenn, M., *et.al.*, Entangled singularity patterns of photons in Ince-Gauss modes. *Phys. Rev. A* **87**, 012326 (2013).

[20] Hendrych, M., Gallego, R., Mičuda, M., Brunner, N., Acín, A., & Torres, J. P., Experimental estimation of the dimension of classical and quantum systems. *Nature Physics* **8**, 588–591 (2012).

[21] Ahrens, J., Badziacedilg, P., Cabello A., & Bourennane M., Experimental device-independent tests of classical and quantum dimensions. *Nature Physics* **8**, 592–595 (2012).

[22] Allen, L., Beijersbergen, M. W., Spreeuw, R. J. C., & Woerdman, J. P., Orbital angular momentum of light and the transformation of Laguerre-Gaussian laser modes. *Phys. Rev. A* **45**, 8185–8189 (1992).

[23] Mair, A., Vaziri, A., Weihs, G., & Zeilinger, A., Entanglement of the orbital angular momentum states of photons. *Nature* **412**, 313-316 (2001).

[24] Fickler, R., *et.al.*, Quantum Entanglement of High Angular Momenta. *Science* **338**, 640 (2012).

[25] Miatto, F. M., Yao, A. M., & Barnett S. M., Full characterization of the quantum spiral bandwidth of entangled biphotons. *Phys. Rev. A* **83**, 033816 (2011).

[26] Salakhutdinov, V. D., Eliel, E. R., & Löffler W. L., Full-Field Quantum Correlations of Spatially Entangled Photons. *Phys. Rev. Lett.* **108**, 173604 (2012).

[27] Monz, T., *et.al.*, 14-Qubit Entanglement: Creation and Coherence. *Phys. Rev. Lett.* **106**, 130506 (2011).

[28] Svozilík, J., Peřina Jr., J., & Torres J. P., High spatial entanglement via chirped quasi-phase-matched optical parametric down-conversion. *Phys. Rev. A* **86**, 052318 (2012).

[29] Barreiro J. T., Langford N. K., Peters N. A., & Kwiat P. G., Generation of Hyperentangled Photon Pairs, *Phys. Rev. Lett.* **95**, 260501 (2005).

[30] Gao, W.-B., *et.al.*, Experimental demonstration of a hyper-entangled ten-qubit Schrödinger cat state. *Nature Physics* **6**, 331 - 335 (2010).

The whole from parts: supplemental material to Studies of Quantum Entanglement in 100 dimensions

Mario Krenn[1,2,*], Marcus Huber[3,4,5,*], Robert Fickler[1,2], Radek Lapkiewicz[1,2], Sven Ramelow[1,2], Anton Zeilinger[1,2,*]
[1] *Institute for Quantum Optics and Quantum Information (IQOQI), Austrian Academy of Sciences, Boltzmanngasse 3, A-1090 Vienna, Austria.*
[2] *Vienna Center for Quantum Science and Technology (VCQ), Faculty of Physics, University of Vienna, Boltzmanngasse 5, A-1090 Vienna, Austria.*
[3] *University of Bristol, Department of Mathematics, Bristol BS8 1TW, U.K.*
[4] *ICFO-Institut de Ciencies Fotoniques, E-08860 Castelldefels (Barcelona), Spain.*
[5] *Fisica Teorica: Informacio i Fenomens Quantics, Departament de Fisica, Universitat Autonoma de Barcelona, E-08193 Bellaterra (Barcelona), Spain.*
[*] *Correspondence on the supplemental material to M.K. (mario.krenn@univie.ac.at), M.H. (marcus.huber@univie.ac.at) and A.Z. (anton.zeilinger@univie.ac.at)*

BOUNDING THE SCHMIDT NUMBER FROM NORMALIZED SUBSPACE CORRELATIONS

The goal of this supplementary is to the determine lower bounds on the Schmidt-number from the sum of all two-dimensional non-normalized subspace correlations in a D dimensional system. It is organized as follows:

- We first introduce the general correlation criterion for normalized subspaces
- We continue by deriving tight lower bounds for the same correlations in non-normalized subspaces
- We then argue using two conjectures for which we have strong numerical evidences, that the maximum for normalized subspaces will be realized by correlations equally distributed over all subspaces
- Finally we derive tight lower bounds for equally distributed correlations in normalized subspaces

Using the following abbreviation

$$|LG_{\pm}\rangle = |k\rangle \ , \tag{S1}$$

where we count all LG modes of $\{n, l\}$, we can represent the performed measurements via the following operators

$$\begin{aligned} \sigma_x^{kl} &:= |k\rangle\langle l| + |l\rangle\langle k| \, , \\ \sigma_y^{kl} &:= i|k\rangle\langle l| - i|l\rangle\langle k| \, , \\ \sigma_z^{kl} &:= |k\rangle\langle k| - |l\rangle\langle l| \, . \end{aligned} \tag{S2}$$

In order to lower bound the dimensionality of entanglement in normalized subspaces we use the following correlation function

$$C(\rho) = \sum_{k<l} \sum_{l=1}^{D-1} g(\rho^{kl}) \, , \tag{S3}$$

where the sum is taken over all ρ^{kl}, the normalized subspace density matrices, where all but two degrees of freedom on both sides are ignored, i.e.

$$\rho^{kl} := \frac{(|k\rangle\langle k| + |l\rangle\langle l|) \otimes (|k\rangle\langle k| + |l\rangle\langle l|)\rho(|k\rangle\langle k| + |l\rangle\langle l|) \otimes (|k\rangle\langle k| + |l\rangle\langle l|)}{N_{kl}} \, , \tag{S4}$$

where N_{kl} is the normalization, such that $\mathrm{Tr}(\rho^{kl}) = 1$, and

$$g(\rho^{kl}) = \mathrm{Tr}\left((\sigma_z^{kl} \otimes \sigma_z^{kl} - \sigma_y^{kl} \otimes \sigma_y^{kl} + \sigma_x^{kl} \otimes \sigma_x^{kl})\rho^{kl}\right) \ . \tag{S5}$$

Comparing these to the correlations on the total state, i.e.

$$f_{kl}(\rho) = \mathrm{Tr}\left((\sigma_z^{kl} \otimes \sigma_z^{kl} - \sigma_y^{kl} \otimes \sigma_y^{kl} + \sigma_x^{kl} \otimes \sigma_x^{kl})\rho\right) , \tag{S6}$$

we can write

$$g(\rho_{kl}) = \frac{f_{kl}}{N_{kl}} , \tag{S7}$$

and thus

$$C(\rho) = \sum_{k<l} \sum_{l=1}^{D-1} \frac{f_{kl}}{N_{kl}} . \tag{S8}$$

It is important to note that of course we only consider contributions from subspaces with a nonzero contribution, i.e. if $N_{kl} = 0$ we set $g_{kl} = 0$.

Lower bounds from non-normalized subspaces

The first step of the witness construction is the determination of the maximal value of $f(\rho) := \sum_{k<l} \sum_{l=1}^{D-1} f_{kl}(\rho)$ for d-dimensional states.

$$\sum_{k<l} \sum_{l=1}^{D-1} f_{kl} \leq \max_{|\psi_d\rangle} f(|\psi_d\rangle\langle\psi_d|) , \tag{S9}$$

where $|\psi_d\rangle = \sum_{i=0}^{d-1} \lambda_i |i_A i_B\rangle$. The first step to achieve this maximization is to realize that

$$f(|\psi\rangle\langle\psi|) \leq \mathrm{Tr}[(2D|\phi_D\rangle\langle\phi_D| + (D-3) \sum_{i=0}^{D-1} |ii\rangle\langle ii|)|\psi\rangle\langle\psi|] , \tag{S10}$$

where $|\phi_D\rangle := \frac{1}{\sqrt{D}} \sum_{i=0}^{D-1} |ii\rangle$ and we got an upper bound via setting all negative contributions to 0. It is well known from Ref. [1] that the maximal overlap of a D-dimensional state with a d-dimensional state $\mathrm{Tr}[|\psi_d\rangle\langle\psi_d||\phi_D\rangle\langle\phi_D|])$ is achieved by $|\psi_d\rangle := \frac{1}{\sqrt{d}} \sum_{i=0}^{d-1} |ii\rangle$. This state also maximizes $\mathrm{Tr}[((D-3) \sum_{i=0}^{D-1} |ii\rangle\langle ii|)|\psi\rangle\langle\psi|]$ such that we can infer that indeed this state achieves the global maximum for $\max_{|\psi_d\rangle} f(|\psi_d\rangle\langle\psi_d|)$ and thus we can directly calculate

$$f(\rho) \leq (2d + (D-3)) . \tag{S11}$$

The structure of the global maximum

Before we proceed to bound the maximum of $C(\rho)$ as a function of D and d we require a few observations:

$$g_{kl} = \frac{4\Re e[\langle kk|\rho|ll\rangle] + \langle kk|\rho|kk\rangle + \langle ll|\rho|ll\rangle - \langle kl|\rho|kl\rangle - \langle lk|\rho|lk\rangle}{\langle kk|\rho|kk\rangle + \langle ll|\rho|ll\rangle + \langle kl|\rho|kl\rangle + \langle lk|\rho|lk\rangle} \leq \frac{4\Re e[\langle kk|\rho|ll\rangle] + \langle kk|\rho|kk\rangle + \langle ll|\rho|ll\rangle}{\langle kk|\rho|kk\rangle + \langle ll|\rho|ll\rangle} , \tag{S12}$$

i.e. monotonically decreasing in the elements $\langle kl|\rho|kl\rangle + \langle lk|\rho|lk\rangle$ for all k and l and thus we conjecture that it is sufficient to maximize over density matrices of the form $\rho = \sum_{k,l} c_{kl} |kk\rangle\langle ll|$ with $\mathrm{Tr}(\rho) \leq 1$. We can numerically confirm this conjecture for low dimensions, but $D \approx 200$ is far out the range of computational feasibility. If the general form of the maximizing density matrices is true this implies that all Schmidt decompositions can be made in computational basis and we can write every vector in the decomposition of the maximizing ρ as $|\psi_\alpha\rangle = \sum_{k\in\alpha} \lambda_k^\alpha |kk\rangle$. This further implies we can decompose the maximizing density matrix as

$$\rho_{max} = \sum_i \sum_{\alpha_i} p_{\alpha_i} |\psi_{\alpha_i}\rangle\langle\psi_{\alpha_i}| , \tag{S13}$$

where $\alpha \subset \{0, 1, (\cdots), D-1\}$ with $|\alpha| \leq d$ denotes the set of dimensions in which the decomposition element is entangled. Without loss of generality we consider the case $|\alpha| = d$, as every density matrix that can be decomposed into Schmidt rank $d' < d$ states is strictly contained in this definition (for some $\lambda_k = 0$). We write (S12) as

$$g_{kl}(\rho) = 4\frac{\sum_{\alpha_i:(k\in\alpha_i)\wedge(l\in\alpha_i)}\sum_i p_{\alpha_i}\lambda_k^{\alpha_i}\lambda_l^{\alpha_i}}{\sum_{\alpha_i:(k\in\alpha_i)\vee(l\in\alpha_i)}\sum_i p_{\alpha_i}((\lambda_k^{\alpha_i})^2+(\lambda_l^{\alpha_i})^2)} + 1\,. \tag{S14}$$

Using the abbreviation $\tilde{\lambda}_k^{\alpha_i} := \sqrt{p_{\alpha_i}}\lambda_k^{\alpha_i}$ we can take the partial derivatives with respect to $\tilde{\lambda}_k^{\alpha_i}$ to find general conditions for all extremal points:

$$\frac{\partial}{\partial\tilde{\lambda}_k^{\alpha_i}}C(\rho) = \sum_{l\in\alpha}\frac{4\tilde{\lambda}_l^{\alpha_i}}{N_{kl}} - 2\tilde{\lambda}_k^{\alpha_i}\sum_l\frac{g_{kl}}{N_{kl}} = 0\,. \tag{S15}$$

Thus

$$\sum_l\frac{g_{kl}}{N_{kl}} = \sum_{l\in\alpha}\frac{4\tilde{\lambda}_l^{\alpha_i}}{N_{kl}2\tilde{\lambda}_k^{\alpha_i}}\,. \tag{S16}$$

Since the left hand side is symmetric in k and l we can conclude that $\tilde{\lambda}_l^{\alpha_i} = \tilde{\lambda}_k^{\alpha_i}$. It then directly follows that

$$\sum_l\frac{g_{kl}}{N_{kl}} = \sum_{l\in\alpha}\frac{4}{2N_{kl}}\,. \tag{S17}$$

And since only the right hand side depends on α, which implies that every partial sum of $\frac{1}{N_{kl}}$ is equal. Thus we can write

$$C(\rho_{max}) \leq \sum_{k<l}\sum_{l=1}^{D-1}\frac{f_{kl}}{N}\,, \tag{S18}$$

where $N = \frac{2}{D}$ and we know from from eq(S11) that $\sum_{k<l}\sum_{l=1}^{D-1} f_{kl} \leq 2d + (D-3)$ we thus get an upper bound

$$C(\rho) \leq Dd + \frac{D}{2}(D-3)\,. \tag{S19}$$

Now we know that all extremal points (of course including all maxima) of the function are upper bounded by this value. Since the normalization of the density matrix does not enter anywhere in the criterion, we can in principle leave all Schmidt coefficients completely unconstrained as only their relative weights enter. The last thing left is to check whether the global maxmimum of the unconstrained function is indeed an extremal point. It is clear that the function can never escape to infinity, for any asymptotic distribution of λ_k^α, since it is algebraically bounded by $\binom{D}{2}$. Still we need to check whether the function cannot asymptotically reach a higher value for some set of $\lambda_k^\alpha \to \infty$. We conjecture that this is the case due to the following reasons: It is easy to see that for any extremal pure state $C(|\psi\rangle\langle\psi|) \leq 3\binom{d}{2} + d(D-d) < Dd + \frac{D}{2}(D-3)$ and an extensive numerical search for $3 < D < 13$ and $d < D$ revealed that indeed the asymptotic regions (corresponding to mixtures of pure state $\sum_i p_i|\psi_i\rangle\langle\psi_i|$) are strictly smaller (and also that all extrema have equally distributed N_{kl}, further strengthening the first conjecture).

Bound for equally distributed correlations

Indeed the previous bounds would be correct for any function that has eqally distributed subspace correlations g_{kl}, as this would imply that each element $f_{kl} = fs_{kl}$ and $N_{kl} = Ns_{kl}$, such that each fraction is a constant $\frac{f}{N}$. Now we can use two inequalities: $\sum_{kl} f_{kl} \leq (2d + (D-3))\mathrm{Tr}[(\sum_{i=0}^{D-1}|ii\rangle\langle ii|)\rho]$ from eq(S11) and the fact that

$$\mathrm{Tr}[(2D|\phi_D\rangle\langle\phi_D| + (D-3)\sum_{i=0}^{D-1}|ii\rangle\langle ii|)\rho] = \mathrm{Tr}[(2D|\phi_D\rangle\langle\phi_D| + (D-3)\sum_{i=0}^{D-1}|ii\rangle\langle ii|)(\sum_{i=0}^{D-1}|ii\rangle\langle ii|)\rho(\sum_{i=0}^{D-1}|ii\rangle\langle ii|)]\,, \tag{S20}$$

and furthermore $\sum_{kl} N_{kl} = 1 + (D-2)\mathrm{Tr}[(\sum_{i=0}^{D-1} |ii\rangle\langle ii|)\rho]$. Now we can get upper bounds for the equal distribution of g_{kl}. The above constraints directly imply:

$$\sum_{k,l} f_{kl} = f \sum_{k,l} s_{kl} \leq (2d + (D-3))\mathrm{Tr}[(\sum_{i=0}^{D-1} |ii\rangle\langle ii|)\rho]$$
$$\sum_{k,l} N_{kl} = N \sum_{k,l} s_{kl} = 1 + (D-2)\mathrm{Tr}[(\sum_{i=0}^{D-1} |ii\rangle\langle ii|)\rho] \tag{S21}$$

The last line implies that $\frac{1}{N}\frac{1}{\sum_{k,l} s_{kl}} \leq \frac{1}{1+(D-2)\mathrm{Tr}[(\sum_{i=0}^{D-1} |ii\rangle\langle ii|)\rho]}$ and thus together we get for the equal distribution that

$$C(\rho) \leq Dd + \frac{D}{2}(D-3)\,. \tag{S22}$$

It is worth pointing out that in general for every $d < D$ this bound is tight, i.e. there exists a mixed state which saturates this bound

$$\rho_d = \frac{1}{\binom{D}{d}} \sum_{\alpha \subset \{0,1,\cdots,D-1\}} |\phi_\alpha^d\rangle\langle\phi_\alpha^d|\,, \tag{S23}$$

where $|\phi_\alpha^d\rangle := \frac{1}{\sqrt{d}} \sum_{k\in\alpha}(|kk\rangle)$ and of course $|\alpha| = d$.

Acknowledgements

MH would like to acknowledge productive discussions with Ariel Bendersky, Stephen Brierley, Jonathan Bohr-Brask, Daniel Cavalcanti, Ottfried Gühne, Karen Hovhannisyan, Claude Klöckl, Milan Mosonyi, Marcin Pawlowski, Martin Plesch, Paul Skrzypczyk and Andreas Winter.

[1] O. Gühne, PhD Thesis